RSC Advances

ROYAL SOCIETY OF CHEMISTRY

www.rsc.org/advances

Chronic toxicity of crude ricinine in rats assessed by ^{1}H NMR metabolomics analysis

Pingping Guo[a†], Dandan Wei[a†], Junsong Wang*[b], Ge Dong[a], Qian Zhang[a], Minghua Yang[a], Lingyi Kong*[a]

[a]*State Key Laboratory of Natural Medicines, Department of Natural Medicinal Chemistry, China Pharmaceutical University, 24 Tong Jia Xiang, Nanjing 210009, PR China. Fax/Tel: 86-25-8327-1405; E-mail: cpu_lykong@126.com*

[b]*Center for Molecular Metabolism, Nanjing University of Science & Technology, 200 Xiao Ling Wei Street, Nanjing 210094, PR China. Tel: 86-25-8431-5512; E-mail: wang.junsong@gmail.com*

*Corresponding author: Prof. Junsong Wang and Prof. Lingyi Kong

† These authors contributed equally to this work

Abstract

Ricinine is a toxic alkaloid contained in the leaves and seeds of *Ricinus communis* L.. It may cause vomiting and various other toxic reactions, including liver and kidney damage, convulsions and hypotension, and even lead to death. In this study, the rats were orally administrated with the extract of castor bean shell (crude ricinine) once a day for eight consecutive weeks to study its chronic toxicity. Urine, serum and kidney samples were collected and subjected to ^{1}H NMR metabolomics analysis. This approach complemented with histopathological inspection and biochemical assay demonstrated that crude ricinine produced obvious nephrotoxicity and severe metabolic alterations in rats. These changes were related with oxidative stress, energy metabolism, amino acid metabolism, renal function and gut bacteria system. This work provided a molecular basis for the chronic toxicity of crude ricinine and showed the power of ^{1}H NMR-based metabolomic approach to study toxicity of drugs dynamically and systematically.

Introduction

Ricinus communis L. (Euphorbiaceae) is a perennial shrub or small arbor distributed throughout temperate and tropical regions. It is an important economical plant because its seeds are the raw material for producing castor oil, which can be used as food additive, flavoring, lubricant, cosmetic ingredient and vulneraria.[1] The seeds of *R. communis* (also named castor bean) contain toxic principles including the alkaloid ricinine[2] and the protein lectins ricin. Ricinine

(Nr-methyl-3-cyano-4-methoxy-2-pyridone) is a neutral alkaloid found mainly in the leaves and castor bean shell of this plant. As an insecticidal agent,[3] ricinine has proven its activity against the Hymenoptera *Atta sexdens rubropilosa*,[4] and the Lepidoptera *Spodoptera frugiperda*.[5] Ricinine may cause vomiting and various other toxic reactions, including liver and kidney damage, convulsions, hypotension, and even lead to death.[6] However, the mechanisms for the toxicity of crude ricinine remain uncertain and have not been fully explored, especially from a holistic perspective.

Metabolomics has been widely applied to examine the progression, generation, and recovery from toxic lesions,[7-9] providing an insight into the integrated function of a complex biosystem at a systemic level.[10] As an unbiased, noninvasive, and rapid analysis technique, ^{1}H NMR has been one of the most widely utilized approaches in metabolomic analyses. ^{1}H NMR spectra of biofluid or tissue are also rich in structural information and could provide a rapid, non-destructive and high-throughput method for metabolomic profiling. Pattern recognition techniques, such as orthogonal signal correction partial least squares discriminate analysis (OSC-PLS-DA) and other statistic analyses could be used to denote and assess holistic biochemical changes.[11, 12] Metabolomics is coincident with the holisticity of traditional Chinese medicine (TCM) and sensitive to stimuli, and thus is suitable for the mechanistic and systematic study of the toxicitites of TCMs,[13-15] which was complicated due to the complex components contained in TCMs.

In our previous study, the toxicity of crude protein ricin from castor bean kernels on rats has been successfully assessed by NMR based metabolomics approach.[16] In

continuation of our studies on the toxic components of castor bean, the chronic toxicity of crude alkaloid ricinine was investigated. Rats were orally administrated with crude ricinine from castor bean shell once a day for eight consecutive weeks. Urine, serum and kidney samples were collected and recorded for ^{1}H NMR spectra, which were analyzed by multivariate OSC-PLS-DA and univariate techniques. This NMR-based metabolomic approach complemented with the biochemical and histopathological observations revealed a series of metabolic pathway perturbations concerning oxidative stress, amino acid metabolism, energy metabolism, renal function and gut bacteria system produced in rats after 8 weeks treatment with crude ricinine.

Experimental

Chemicals, reagents and herbal materials

The seeds of *R. communis* were purchased from Anguo Qirui Chinese Herbal Medicine Company (Hebei, China) and identified by Professor Mian zhang, Department of Medicinal Plants, China Pharmaceutical University, Nanjing, China. The voucher specimen was deposited in Department of Natural Medicinal Chemistry, China Pharmaceutical University. The kits of blood urea nitrogen (BUN), urine urea nitrogen (UUN), serum creatinine (SCR), urine creatinine (UCR), urine protein (UP), urine N-acetyl-β-D-glucosaminidase (NAG), and ELISA Assay kit of rat retinol binding protein (RBP) were bought from Nanjing Jiancheng Bioengineering Institute (Nanjing, China). Deuterium oxide (D_2O, 99.9 %) was purchased from Sigma

Chemical Co. (St. Louis, MO, USA). Distilled water was purified using a Milli-Q system (Millipore, Bedford, MA, USA).

Herbal material process

Dried and crushed castor bean shell (3600 g) was extracted with 50% ethanol (1:8 w/v) under reflux for 2 h for three times. The filtrates were combined, concentrated under reduced pressure and lyophilized to give yellow crude extracts (9.5% yield). The dried extracts were suspended in 0.5% (w/v) sodium carboxymethylcellulose (CMC-Na) and the doses were calculated as raw material weights for animal experiments. Ricinine from the yellow residue was indentified by ^{1}H-NMR and LC-MS.

Analysis of ricinine by ^{1}H NMR and LC-MS

^{1}H NMR spectrum of ricinine was recorded on a Bruker Avance 500 MHz spectrometer (Bruker Biospin, Germany).

The HPLC analyses were performed using an Agilent 1290 HPLC instrument (Agilent, Waldbronn, Germany) equipped with a binary pump, an online egasser, an autosampler and a thermostatically controlled column compartment. The samples were separated on an Agilent ZorBax Eclipse XDB-C_{18} column (4.6 × 220 mm, 5 μm, Agilent Corporation, Santa Clara, CA, USA). The mobile phase consisted of methanol (solvent A) and water (solvent B) using a gradient elution according to the following profile: 0.0-10.0 min, 10~25% B; 10.5-16.5 min, 50% B; 17.0-25.0 min, 70-100% B. The flow rate was 1 mL/min and the column temperature was set at 30 °C.

Detections were performed using an Agilent 6520 QTOF mass spectrometer (Agilent Corporation), which was connected to the Agilent 1290 UHPLC instrument via an ESI interface. The operating parameters were as follows: drying gas (N_2); flow rate, 8.0 L/min; temperature, 320 °C; nebuliser, 35 psig; capillary, 4000 V; fragmentor, 175 V; skimmer, 65 V; OCT RF V, 750 V. All the operation, acquisition and analysis of data were performed using Masshunter workstation software Version B.04.00 (Agilent). The sample was analysed in positive ion mode. The $[M+H]^+$ ion of interest in the positive mode was selected as the precursor ion. The collision energy (CE) was adjusted from 30 to 55 eV and the mass range was from *m/z* 100 to 1000.

Animals and treatment

A total of 36 male Sprague-Dawley rats (220 ± 10 g) were purchased from Experimental Animal Center of Yangzhou University (Yangzhou, China). Rats were housed in a climate-controlled room at a temperature of 25±3 °C and a relative humidity of 50±10%, with a 12 h light/12 h dark cycle. Food and tap water were provided *ad libitum*. The rats were acclimatized for one week in stainless steel wire-mesh cages before treatment. The study was approved by the Jiangsu Animal Care and Use Committee and followed the national and institutional rules considering animal experiments.

Rats were randomly divided into three groups, 12 animals each, as follows: those administered with crude ricinine corresponding to a raw castor bean shell at a dose of 10 g and 4 g /(kg day) as high dose group (HD) and low dose group (LD), respectively,

and those treated with the same volume of CMC-Na as control group (NC). The oral gavage administration was adopted and performed once a day for eight consecutive weeks.

Collection and preparation of samples

Urine samples were collected into vials using metabolic cages overnight (from PM 8:00 to AM 8:00): the rats were deprived of food to avoid solid debris pollution, but were allowed free access to tap water. The collected urine samples were centrifuged at 12,000 rpm for 10 min to aid the settling of coarse material and then were kept at −80 °C before use.

Blood samples were taken from ocular veins of rats after 12 h fasting on week 0, 1, 3, 5 and 8 after the treatment. The serum samples were obtained by centrifugation (12,000 rpm, 10 min, 4 °C), stored at −80 °C before biochemical analysis.

Histopathology

At the end of the experiment, rats were fasted overnight and then anaesthetized by intraperitoneal injection (i.p.) of 3.5% chloralhydrate (350 mg/kg body weight). Kidney and liver were quickly removed, then rinsed with cold PBS and immersed in 10% neutral-buffered formaldehyde for 24 h, embedded in paraffin, and sliced into 5 μm thickness. The sliced sections were stained with hematoxylin and eosin (H&E), and examined by light microscopy (200× and 400×).

157 **Biochemistry and kidney index**

158 To assess renal function, the concentrations of BUN and SCR in serum, and UUN,
159 UCR, UP, NAG and RBP in urine were determined, and the kidney index (kidney
160 weight/body weight) was calculated.

161

162 **Sample preparation for NMR recording**

163 Frozen kidney tissues (500-600 mg) were homogenized in a mixture of volumetric
164 equivalent acetonitrile and water (5 mL/g tissue) in an ice/water bath and centrifuged
165 at 12,000 g for 10 min at 4 °C. The supernatant was collected and concentrated under
166 a stream of nitrogen and lyophilized. Dried kidney extracts were reconstituted in 600
167 μL D_2O (0.2 M Na_2HPO_4 and 0.2 M NaH_2PO_4, pH 7.0, containing 0.05 % TSP). To
168 400 μL urine or 300 μL serum samples, 200 or 300 μL D_2O were added, respectively,
169 to minimize NMR shift variation due to the pH discrepancy.
170 The suspension was vortexed, and then centrifuged at 12000 rpm for 10 min to remove
171 any precipitates. Aliquots of the resulting supernatant (450 μL) was pipetted into 5 mm
172 NMR tubes. TSP was used as the chemical shift reference (δ_H = 0.00), and D_2O
173 provided the field frequency lock signal.

174

175 **^{1}H NMR spectrometry**

176 ^{1}H NMR spectra of urine and kidney samples were acquired at 298 K on a Bruker
177 Avance 500 MHz spectrometer with a Bruker 5 mm probe, using a modified nuclear
178 Overhauser enhancement spectroscopy (NOESY) pulse sequence to suppress the

residual water signal. Free induction delays (FIDs) were collected with 1024 transients into 32768 data points using a spectral width of 10000 Hz with a relaxation delay of 2 s, an acquisition time of 4 s, and a mixing time of 100 ms. All spectra were zero-filled to 64 k data points, and a line-broadening of 0.5 Hz was applied.

^{1}H NMR spectra of serum were recorded on a Bruker Avance 500 MHz spectrometer using the Carr-Purcell-Meiboom-Gill (CPMG) pulse sequence to attenuate the NMR signals of any residual proteins, with irradiation at water frequency during both a recycle delay of 2 s and a mixing time of 100 ms. Typically, 128 free induction decays (FIDs) were collected into 64 K points using a spectral width of 10000 Hz, an acquisition time of 1.36 s and a relaxation delay of 1.5 s. The Fourier transformed NMR spectra were manually phased and automatically baseline corrected.

Data analysis

^{1}H NMR spectra were converted to ASCII files using MestReNova (Version 8.0.1, Mestrelab Research SL), and aligned based on least square minimization with shift corrected by the TSP signal. The spectral range of δ 0.40-4.16 and δ 5.7-8.5 for urine, δ 0.60-4.25 for serum, and δ 0.60-4. 60 and δ 5.10-9.50 for kidney were binned into integrated segments of equal width of 0.005 ppm using the R software (http://cran.r-project.org/). The region of 4.16-5.7 ppm in the urine spectra and 4.60-5.10 ppm in kidney spectra were excluded to remove those regions affected by residual water. All the spectra were normalized by probabilistic quotient normalization. The data were centered and pareto-scaled before multivariate analysis. A

non-supervised principal components analysis (PCA) revealed no obvious clustering of groups (data not shown). A supervised OSC-PLS-DA method was then carried out, which could remove systematic variations unrelated to interested status through an orthogonal filter. Repeated 2-fold cross-validation (20 times) was applied in the OSC-PLS-DA model; the validity of the models against overfitting was assessed by the parameter R^2, and the predictive ability was described by Q^2. Classification performance was evaluated by analyzing receiver operating characteristic (ROC) plots generated using the R-package ROCR (http://rocr.bioinf.mpi-sb.mpg.de). For each classification, the average prediction accuracy given as the arithmetic mean ± SD of the individual results and the area under the ROC curve (AUROC) was given. The integration areas of the detected metabolites with potential differentiating ability were first tested for their normality of the distribution. If the distribution followed the normality assumption, a parametric Student's t-test was applied; otherwise, a nonparametric Mann-Whitney test was performed to detect statistically significant metabolites that were increased or decreased between groups over time. Data were expressed as mean ± SD and $P < 0.05$ was considered statistical significant.

Results

Identification of ricinine by ^{1}H NMR and LC-MS

Ricinine was indentified by ^{1}H NMR and LC-MS. ^{1}H NMR (500 MHz, DMSO): δ 8.10 (1H, d, J = 7.8 Hz, 6-H), 6.43 (1H, d, J = 7.8 Hz, 5-H), 3.98 (3H, s, OCH_3), 3.43 (3H, s, CH_3). The results are consistent with those reported in the literature[6]. Accord

ing to the precursor ion $[M+H]^+$ of 165.0659, corresponding to an elemental composition $C_8H_8N_2O_2$, the signal of response at an acquisition time of 9.818 min was identified to be ricinine (Fig. S1).

Histopathology

Livers and kidneys of rats exposed to crude ricinine were examined for histopathology. The kidney section of the NC rat showed apparently normal structure in renal glomerulus and tubule (Fig. 1A and D). The kidney of HD rats showed significant tubular epithelial cell degeneration (edema) and diaphanous tubular cast (Fig. 1C and F); the kidney of LD rats showed a moderate degeneration (Fig. 1B and E). No significant pathological changes were observed in the liver tissues of dosed rats.

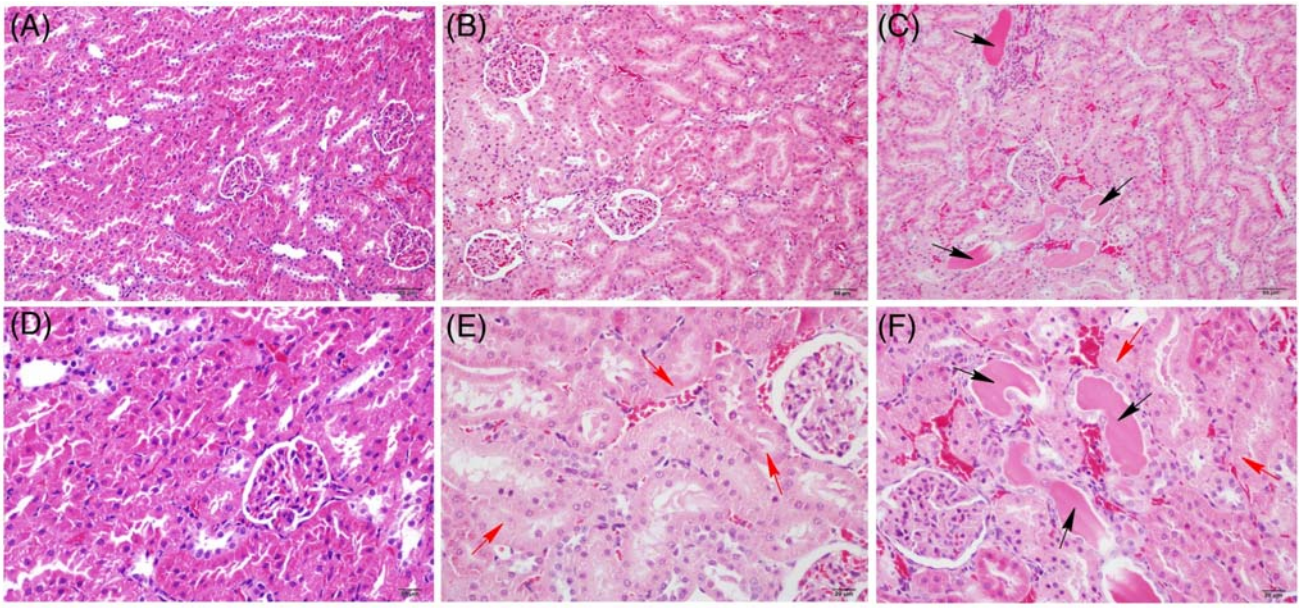

Fig.1 Histopathological photomicrographs of rat kidney (A, B and C ×200; D, E and F ×400) manifested from hematoxylin-eosin (HE) staining. Kidney of HD rats (C and F) showed severe tubular epithelial cell edema (red arrow) and diaphanous tubular cast (black arrow) as compared with those of NC (A and D), and the kidney of LD rats (B and E) showed moderate edema (red arrow).

Biochemistry

The levels of BUN, UUN, SCR, UCR, UP, NAG, and RBP were measured, and the kidney index of all groups of rats was calculated to assess kidney function (Fig. 2). BUN in dosed groups did not show significant difference on week 1, but increased gradually from week 3, reaching the maximal difference in week 8. SCR followed a similar but delayed trend as compared with BUN: its level in dosed groups showed no significant difference from the control group from week 1 to week 3, turned to increase from week 5, reaching the maximum on week 8. UUN and UCR of dosed groups showed somewhat fluctuation throughout the experiments: decreased markedly on week 1 (early stage) and week 8 (late stage) but kept at nearly same levels in other time periods. The UP, NAG and RBP concentrations of dosed groups showed significant increase at all time periods, but alleviated from week 3 to week 5. However, the kidney index of dosed groups only showed slight decrease, without significance.

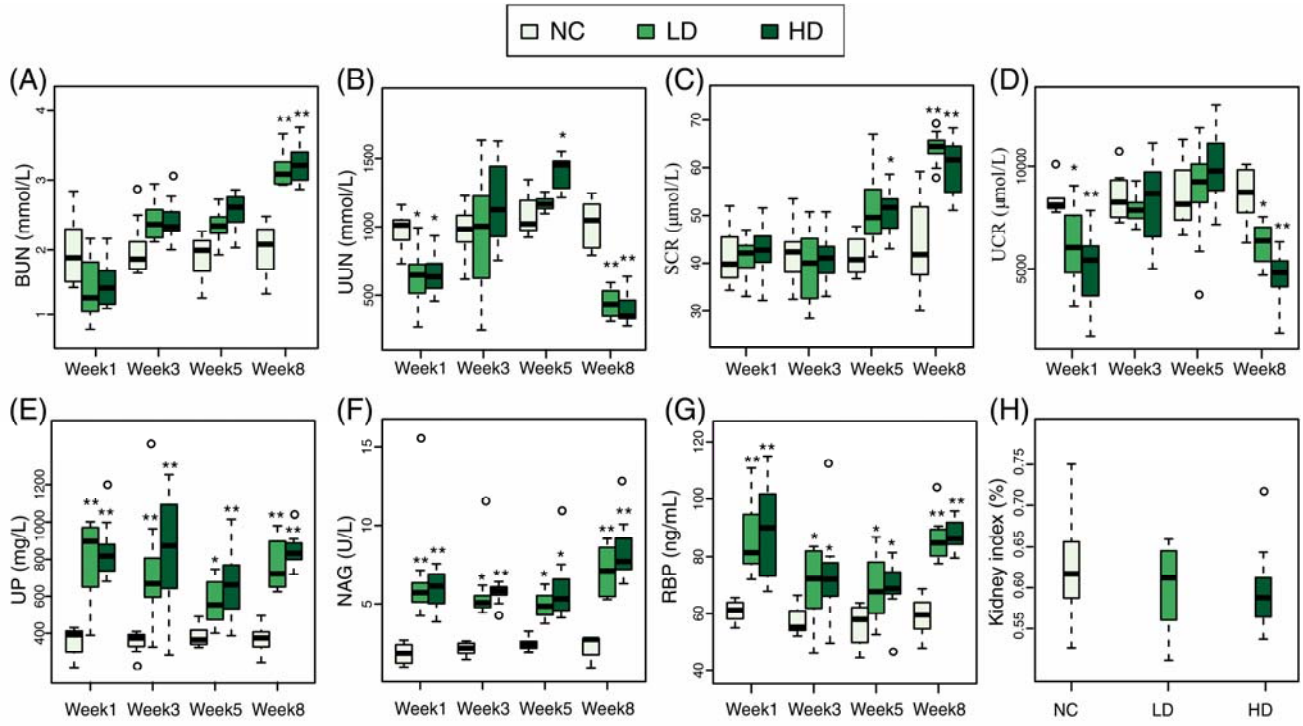

Fig.2 Boxplots for values of BUN (A), UUN (B), SCR (C), UCR (D), UP (E), NAG (F), RBP (G) and kidney index (H) in the control and dosed groups. The bottom of each box, the line drawn in the box and the top of the box represent the 1st, 2nd, and 3rd quartiles, respectively. The whiskers extend to ± 1.5 times the interquartile range (from the 1st to 3rd quartile). Outliers are shown as open circle. All values are mean ± SD (n = 8). *P < 0.05 and ** P < 0.01 vs NC.

^{1}H NMR spectra analyses

Typical ^{1}H NMR spectra of urine, serum and kidney extract for HD group and NC group on week 8 were presented in Fig. 3, with major metabolites labeled. Aided by STOCSY technique, their assignments (Table 1) were made by referencing reported data and searching publicly accessible metabolomic databases, such as HMDB (http://www.hmdb.ca), MMCD (http://mmcd.nmrfam.wisc.edu) and ECMDB (http://www.ecmdb.ca).

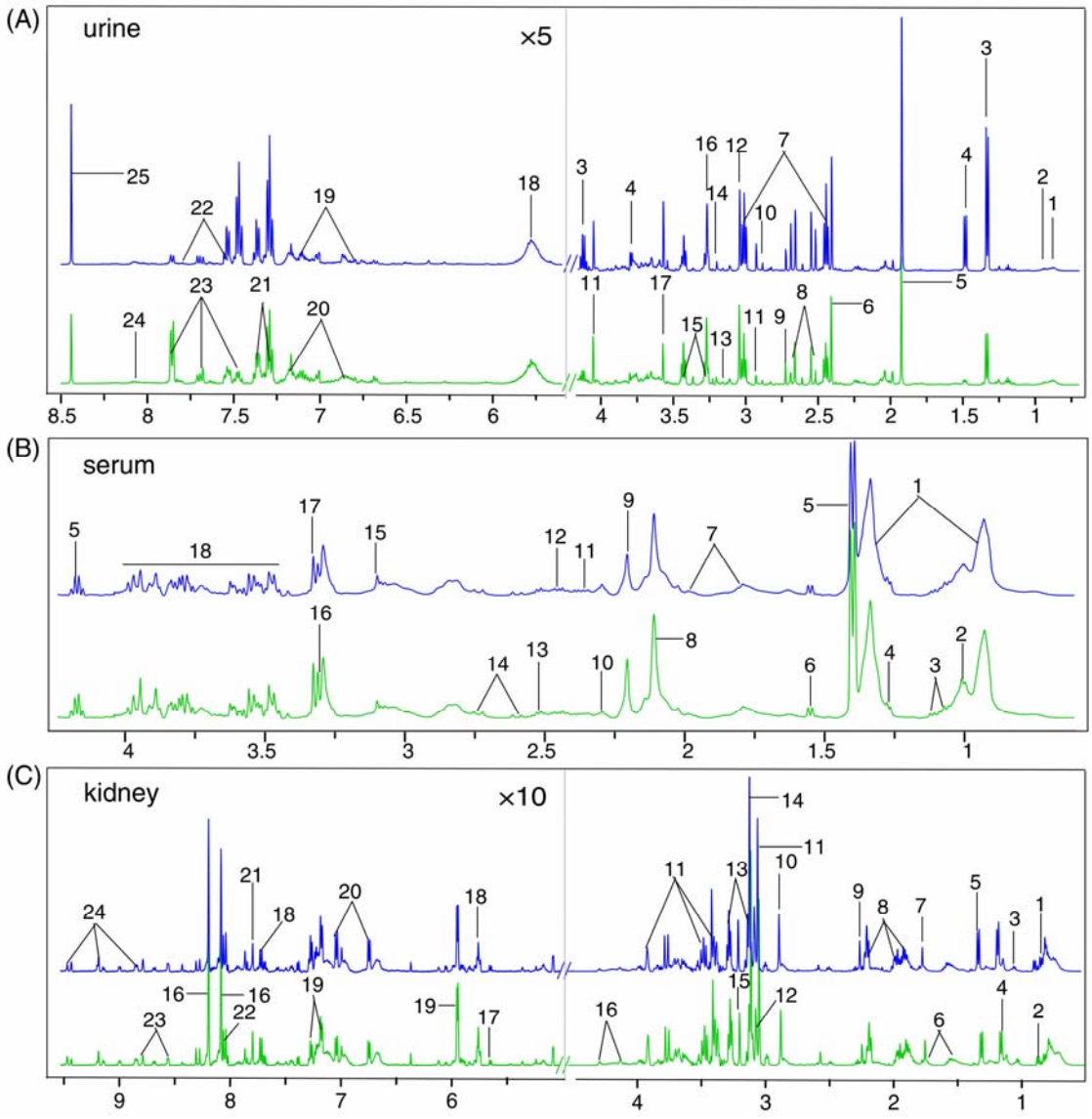

Fig.3 Typical 500 MHz ^{1}H NMR spectra of the urine (A), serum (B) and kidney (C) on week 8 from HD group and NC group. Metabolites in urine: 1, Isoleucine/Leucine; 2, Valine; 3, Lactate; 4, Alanine; 5, Acetate; 6, Succinate 7, 2-oxoglutarate; 8, Citrate; 9, Dimethylamine; 10, Trimethylamine; 11, N,N-dimethylglycine; 12, Creatinine; 13, Choline; 14, Phosphocholine; 15, Taurine; 16, Trimethylamine-N-oxide; 17, Glycine; 18, Urea; 19, 4-hydroxyphenyllactate; 20, Tyrosine; 21, Phenylalanine; 22, Hippurate; 23, Benzoate; 24, Trigonelline; 25, Formate. Metabolites in serum: 1, Lipoprotein (LDL/VLDL); 2, Leucine/Isoleucine; 3, Valine; 4, β-hydroxybutyrate; 5, Lactate; 6, Alanine; 7, Arginine; 8, N-acetyl-glycoproteins; 9, O-acetyl-glycoproteins; 10, Glutamate; 11, Glutamine; 12, Acetoacetate; 13, Pyruvate; 14, Citrate; 15, Creatinine; 16, Taurine; 17, Trimethylamine-N-oxide; 18, Glucose. Metabolites in kidney: 1, Leucine/Isoleucine; 2, Valine; 3, β-hydroxybutyrate; 4, Lactate; 5, Alanine; 6, Arginine; 7, Acetate; 8, Glutamate; 9, Acetoacetate; 10, Creatinine; 11, Choline; 12, Phosphocholine; 13, Taurine; 14, Trimethylamine-N-oxide; 15, scyllo-Inositol; 16, myo-Inositol; 17, adenosine; 18, Uridine; 19, Tyrosine; 20, Phenylalanine; 21, Xanthine; 22, Hypoxanthine; 23, Nicotinamide; 24, Nicotinamide mononucleotide.

Table 1 Identified metabolites from different groups with fold change and P value.

	No.	Mebabolite	Assignments	Chemical shift (ppm)	FC^1_H	P^2_H	FC^1_L	P^2_L
Urine	1	Leucine/Isoleucine	CH_3	0.93(t),1.02(d)	1.28		1.86	*
	2	Valine	CH_3	0.97(d),1.07(d)	1.04		1.07	
	3	Lactate	CH_3,CH	1.35(d),4.15(q)	0.57	*	0.6	*
	4	Alanine	CH_3,CH	1.51(d),3.78(q)	0.67	*	0.7	
	5	Acetate	CH_3	1.93(s)	0.44	**	0.39	**
	6	Succinate	CH_2	2.43(s)	1.19		1.07	
	7	2–Oxoglutarate	CH_2	2.45(t),3.02(t)	1.53	*	1.5	*
	8	Citrate	CH	2.60(AB),2.72(AB)	1.96	***	2.09	***
	9	Dimethylamine	CH_3	2.73(s)	1.2		1.06	
	10	Trimethylamine	CH_3	2.88(s)	0.32	**	0.27	***
	11	Dimethylglycine	CH_3	2.93(s)	0.95		0.94	
	12	Creatinine	CH_3,CH_2	3.03(s),4.05(s)	1.73	**	1.39	*
	13	Choline	$N(CH_3)_3$–CH_2	3.19(s),3.51(m)	0.78		0.68	*
	14	Phosphocholine	CH_3	3.21(s)	1.27	*	1.11	**
	15	Taurine	SO_3–CH_2-CH_2–NH_2	3.27(t),3.42(t)	1.73	**	1.51	**
	16	Trimethylamine N-oxide	CH_3	3.26(s)	1.9	***	1.55	**
	17	Glycine	CH_2	3.57(s)	0.96		1.1	
	18	Urea	NH_2	5.80(br)	3.65	***	2.08	***
	19	4–hydroxyphenyllactate	CH	6.85(d),7.16(d)	0.66		0.47	**
	20	Tyrosine	CH	6.89(m),7.18(m)	1.62	**	1.18	
	21	Phenylalanine	CH	7.32(m),7.40(m)	0.5	**	0.68	*
	22	Hippurate	CH_2,CH	3.94(d),7.55(m),7.83(m)	1.5	*	1.39	
	23	Benzoate	CH	7.47(dd),7.54(t),7.86(d)	0.9		0.84	
	24	Trigonelline	CH	8.08(t)	1.58	**	1.13	
	25	Formate	CH	8.44(s)	0.19	***	0.32	**
Serum	1	Lipoprotein(LDL/VLDL)	CH_2	0.89 (m), 1.20-1.30 (m)	1.02	*	1.05	***
	2	Leucine/Isoleucine	δCH_3, δCH_3	0.93 (t), 1.02 (d)	0.98		1.03	
	3	Valine	γCH_3, γCH_3, βCH, αCH	1.03 (d), 1.08 (d)	0.90		0.93	*
	4	β-hydroxybutyrate	γCH_3, βCH	1.26 (d), 4.23 (m)	0.81	**	1.01	
	5	Lactate	CH_3, CH	1.39 (d), 4.15 (q)	1.25	**	1.15	**
	6	Alanine	βCH_3, αCH	1.55 (d), 3.78 (q)	1.10		1.02	
	7	Arginine	γCH_2, βCH_2	1.78 (m), 1.95 (m)	1.01		1.00	
	8	N-acetyl-glycoproteins	CH_3	2.09 (s)	0.76	***	0.89	***
	9	O-acetyl-glycoproteins	$OHCHCH_3$	2.19 (s)	0.63	***	0.81	***
	10	Glutamate	βCH_2, γCH_2	2.08 (m), 2.46 (m)	0.86	***	0.94	
	11	Glutamine	βCH_2, γCH_2	2.13 (m), 2.54 (m)	0.97	*	0.99	
	12	Acetoacetate	CH_3	2.30 (s)	0.61	***	0.66	**
	13	Pyruvate	βCH_3	2.35 (s)	0.95		0.96	
	14	Citrate	$1/2CH_2$, $1/2CH_2$	2.60 (AB), 2.75 (AB)	1.03	*	0.99	
	15	Creatinine	CH_3, CH_2	3.10 (s), 4.05 (s)	0.88	*	0.91	
	16	Taurine	SO_3-CH_2	3.29 (t)	1.10	**	1.05	
	17	Trimethylamine N-oxide	CH_3	3.34 (s)	1.22	***	1.22	***
	18	Glucose	CH	3.45-4.0 (m)	1.13	***	1.02	
Kidney	1	Isoleucine/Leucine	δCH_3,βCH_3	0.91 (t), 1.02 (d)	0.80	**	0.82	**
	2	Valine	γCH_3,γCH_3	0.96 (d), 1.06 (d)	0.76	**	0.76	**
	3	β-hydroxybutyrate	γCH_3, βCH	1.12 (d), 4.23 (m)	1.06		1.12	
	4	Lactate	CH_3,CH	1.25 (d), 4.15 (q)	0.64	***	0.68	*
	5	Alanine	βCH_3,αCH	1.41 (d), 3.78 (q)	0.90	**	0.89	
	6	Arginine	CH_2,CH_2	1.64 (m), 1.83 (m)	0.80	*	0.82	*
	7	Acetate	CH_3	1.75 (s)	0.80	*	0.90	
	8	Glutamate	βCH_2, γCH_2	1.98 (m), 2.26 (m)	0.90	**	0.89	*
	9	Acetoacetate	CH_3	2.31 (s)	0.80	***	0.74	***
	10	Creatinine	CH_3,CH_2	2.96 (s),4.07 (s)	0.98		1.02	
	11	Choline	$N(CH_3)_3$,N–CH_2	3.12 (s), 4.07 (s)	1.35	*	1.32	
	12	Phosphocholine	CH_3	3.15 (s)	1.03	*	1.01	
	13	Taurine	SO_3–CH_2,CH_2–NH_2	3.20(t),3.35(t)	1.05		1.02	
	14	Trimethylamine N-oxide	CH_3	3.2(s)	1.02		1.02	
	15	scyllo-Inositol	CH	3.26(s)	0.98		0.99	
	16	myo-Inositol	CH	3.35 (t), 3.48 (t), 3.55 (t), 3.99 (s)	1.16	***	1.16	***
	17	Adenosine	CH_3	4.21- 4.35 (m), 6.02 (d), 8.16 (s), 8.27 (s)	1.22	***	1.20	***
	18	Uridine	CH_2, CH	5.88 (m), 7.79 (d)	1.22	**	1.15	**
	19	Tyrosine	CH	6.91 (d),7.20 (d)	0.69	***	0.72	***
	20	Phenylalanine	CH	7.32 (d),7.42 (m)	0.83	***	0.84	**
	21	Xanthine	CH	7.93 (s)	0.68	***	0.77	*
	22	Hypoxanthine	CH	8.20 (s), 8.22 (s)	1.16	*	1.16	*
	23	Nicotinamide	CH	8.55 (m), 8.77 (m)	0.90	**	0.89	*
	24	Nicotinamide mononucleotide	CH	8.82 (d), 9.22 (d), 9.51 (s)	0.85	*	0.89	

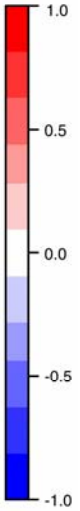

Multiplicity: s, singlet; d, doublet; t, triplet; q, quartet; m, multiplet; br, broad singlet.

The superscript "1" and "2" means fold change and P value respectively (* P< 0.05, ** P< 0.01 and *** P< 0.001); the subscript "H" and "L" means NC vs HD and NC vs LD respectively.

Color coded according to $\log_2$(fold change) using the color bar labeled at the right side.

OSC-PLS-DA score trajectory plot of all groups at all time periods

In order to dynamically explore the chronic effect of crude ricinine on the metabolic pattern of dosed rats, OSC-PLS-DA model was constructed to analyze all the urine (R^2

= 0.80, Q^2 = 0.56, $P < 0.005$) and serum (R^2 = 0.51, Q^2 = 0.29, $P < 0.005$) data acquired from control and treatment groups on week 1, 3, 5 and 8. The trajectory plot (Fig. 4) exhibited a good separation between HD and NC group, with LD group in between, showing an apparent dose-dependent toxic effect of crude ricinine. A radical alteration in metabolomic profiles of dosed groups happened on week 1, reflecting a prompt response of the body to the dosing. The metabolomic changes in dosed rats attenuated from week 1 to week 3, and then this trend was terminated from week 3 onwards, decreased to the minimum on week 5, but finally increased to another maximum on week 8. Serum data showed a similar pattern, but a delayed alleviation from week 5. This fluctuation of metabolic pattern change showed a complex response of the organism to counteract the toxicity of the dosing.

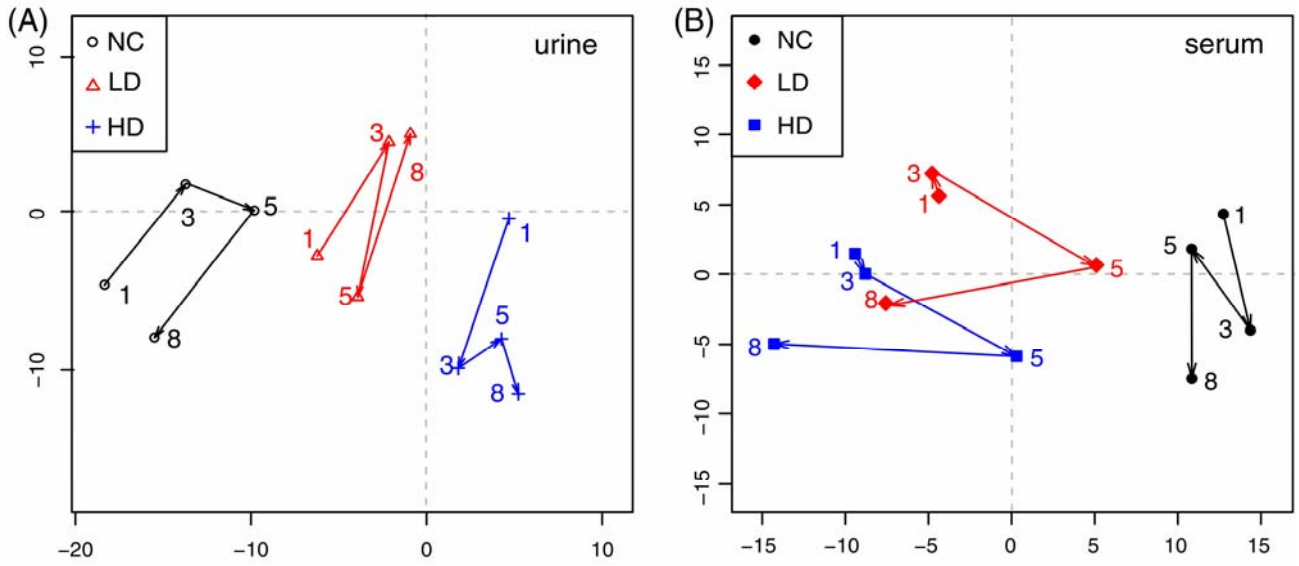

Fig.4 Score trajectory plot of urine (A) and serum (B) from OSC-PLS-DA analysis of HD, LD and NC groups (1, 3, 5, 8 means time period)

^{1}H NMR metabolomics profiles of HD and NC group on week 8

Considering the dose-dependent effects of crude ricinine, the NMR data from HD and

NC rats of week 8 were further analyzed by OSC-PLS-DA to denote the chronic toxic effects of crude ricinine on rats in the long run. 2CV was used to validate the statistical significance of each model in order to avoid overfit. High values of R^2 and Q^2 of OSC-PLS-DA of urine, serum and kidney data (Fig. 5A, C and E) indicated satisfactory models with reliable predictive ability and minimal classification error. The value of AUROC of urine, serum and kidney data were 0.886, 0.999 and 0.994 respectively (Fig. 5B, D and F), showing the satisfactory classifier performance of the OSC-PLS-DA model. The score plots of PC1 versus PC2 (Fig. 6A, C and E), where each point represented one sample, revealed a clear separation of HD group from NC group along PC1. In order to identify the spectral bins that were responsible for the inter-class differences, the loadings S-plot for the first component were generated (Fig. 6B, D and F). The S-plot is a scatter plot that visualize both the covariance (X axis) and correlation (Y axis) structure of loading profiles, thus would be helpful for filtering interesting metabolites in the projection, and for lowering the risk of false positive in metabolite selection. The significant metabolites increased in HD group were in the higher-right quadrant and the decreased in the lower-left quadrant. The corresponding loadings plot color-coded with correlation coefficients of metabolites visualized the variables responsible for the separation between HD and NC group. The weight of a variable in the discrimination was given by the square of its correlation coefficient (r^2), which was color coded from zero in blue to high values in red. The S-plot and color coded loadings plot revealed a large number of metabolites contributing to the clustering of groups. Compared with NC, these findings were

observed in HD group: elevated levels of lactate, alanine, acetate, phenylalanine, TMA (Trimethylamine), 4-HPLA (4-hydroxyphenyllactate), formate in urine; elevated levels of leucine/isoleucine, valine, 3-HB (β-hydroxybutyrate), N-acetyl-glycoproteins, O-acetyl-glycoproteins, acetoacetate, pyruvate, glutamine, glutamate, citrate, creatinine in serum; elevated levels of leucine/isoleucine, valine, lactate, arginine, creatinine, tyrosine, phenylalanine, xanthine in kidney; reduced levels of tyrosine, hippurate, succinate, 2-OG (2-oxoglutarate), citrate, taurine, TMAO (Trimethylamine-N-oxide), TRG (Trigonelline), urea and creatinine in urine; reduced levels of LDL/VLDL, lactate, alanine, arginine, taurine, TMAO, glucose in serum; reduced levels of choline, myo-inositol, adenosine, uridine, hypoxanthine in kidney. These important differential metabolites selected based on loadings plot and S plot of OSC-PLS-DA were further tested for their between-group difference and found to be mostly significant as visualized in the fold change plot (Fig. S2).

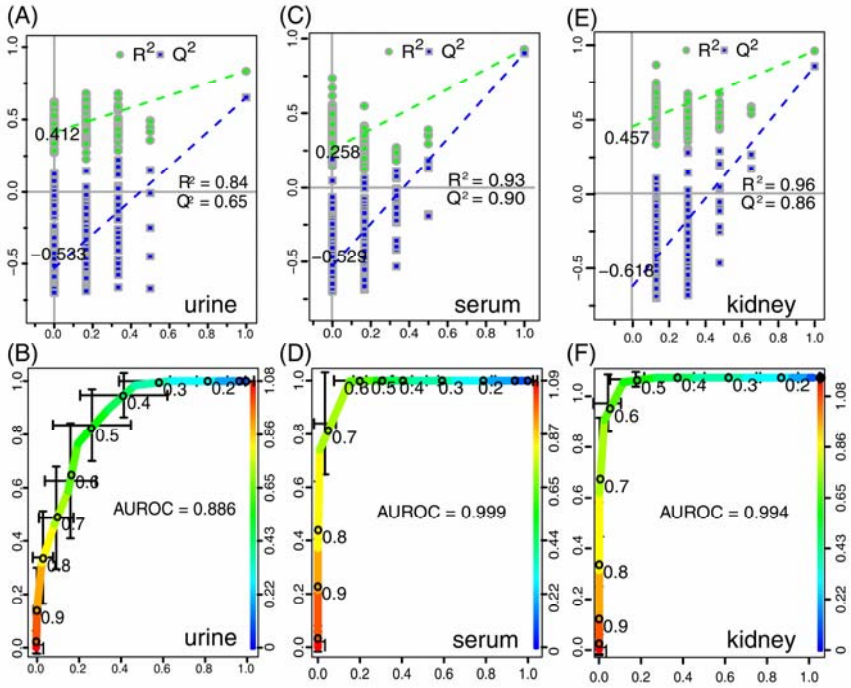

Fig. 5 OSC-PLS-DA scatter plot from urine (A), serum (C) and kidney (E) of statistical validation

obtained by 200 times permutation test, with R^2 and Q^2 values in the vertical axis, the correlation coefficients (between the permuted and true class) in the horizontal axis, and OLS line for the regression of R^2 and Q^2 on the correlation coefficients. Receiver operating characteristic (ROC) curves of classifier performance of OSC-PLS-DA model on ^{1}H NMR data of of urine (B), serum (D) and kidney (F), with the area under the receiver operating characteristic curves (AUROC) labeled. The X-axis denotes the false positive rate, the Y-axis the true positive rate. After repeated 2-fold cross-validation 20 times, the AUROC was calculated.

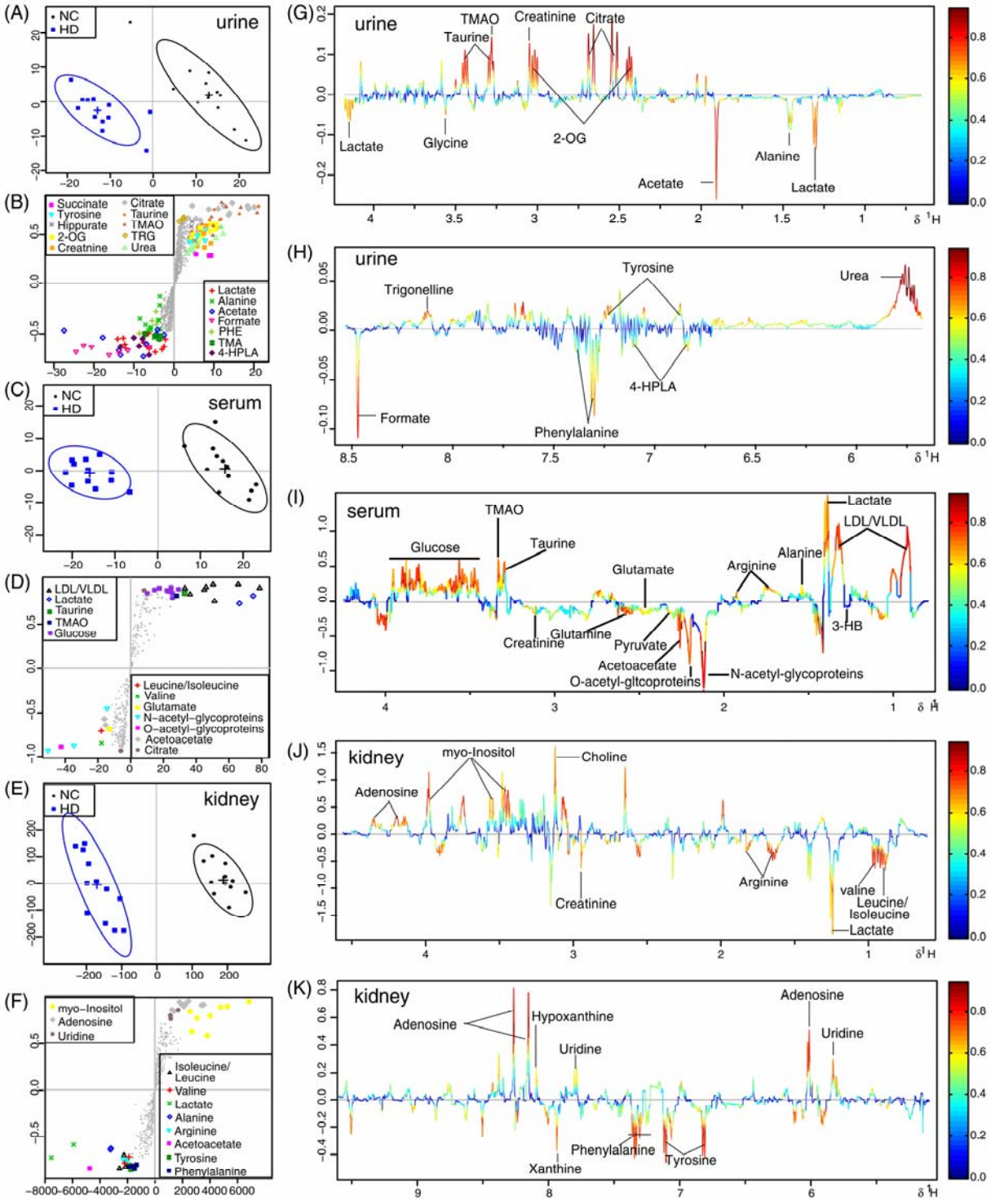

Fig.6 Scores plot (A, C, E), S-plot (B, D, F) and loadings plot with the metabolites labeled (G-K) corresponding to the OSC-PLS-DA analysis of urine (A, B, G, H), serum (C, D, I) and kidney (E, F, J, K) from HD and NC group (n = 12 for each group) on week 8: Loadings plot was color-coded with the correlation coefficients of variables in the OSC-PLS-DA model with blue the least important metabolic changes and red the most important. Positive peaks indicate a relatively decreased metabolite level in dosed groups, while negative peaks indicate an increased metabolite level in HD group.

Metabolite pathway analysis

Potential biomarkers selected based on OSC-PLS-DA loadings plot, S-plot and fold change plot were subjected to pathway analysis using MetPA (http://www.metaboanalyst.ca) to identify biologically meaningful metabolic patterns and the most relevant pathways. A hypergeometric test using over-representation analysis and pathway topology analysis (Table S1, S2 and S3) indicated that valine, leucine and isoleucine biosynthesis, phenylalanine, tyrosine and tryptophan biosynthesis, phenylalanine metabolism, synthesis and degradation of ketone bodies and TCA cycle were disturbed in HD group rats (Fig. S3).

Discussion

The chronic toxicity of crude ricinine in rats was firstly investigated by histopathological inspection and biochemical evaluation. The kidney of dosed rats showed marked tubular epithelial cell edema and diaphanous tubular cast. Urinary excretion of UP, NAG and RBP was markers of tubular damage[17] and alternative indicators of nephropathy,[18] and evaluation of BUN and SCR concentrations were indicators of renal dysfunction.[19] Urinary RBP could be used for early detection of renal tubular dysfunction, sensitively reflecting the damage extent of the renal

proximal tubule; urinary NAG was a sensitive indicator of renal impairment, particularly on renal tubular ischemic and necrosis. The significantly increased urinary UP, NAG and RBP after dosing indicated renal damage induced by ricinine. BUN and SCR in dosed groups were significantly increased on week 8 while UUN and UCR in dosed groups were decreased remarkably on week 1 and 8, suggesting an obvious chronic dysfunction of kidney.

To investigate the variations of endogenous metabolites in rats administered with crude ricinine, a ^{1}H NMR-based metabolomics approach on urine, serum and kidney samples was adopted to explore potential biomarkers and the affected metabolic pathways for the first time. OSC-PLS-DA analysis of urine and serum NMR data of the three groups at all time periods was performed. The metabolic status of rats was greatly changed by crude ricinine in a dose-dependent manner, peaked at the early (week 1) and late stage (week 8) of the experiments. NMR data of urine, serum and kidney from HD and NC group on week 8 were then further analyzed and revealed a series of metabolic pathway perturbations including oxidative stress, energy metabolism perturbation, renal damage and gut bacteria disruption.

Oxidative stress, a serious imbalance between the generation of reactive oxygen species (ROS) and antioxidant defenses, has been demonstrated to be a major mechanism involved in shock, inflammation, and ischemia/reperfusion injury[20] and the toxicities of some toxins.[21-25] Compared with NC rats, decreased levels of serum glutamate and glutamine were observed in HD rats. As precursors of the major natural antioxidant glutathione (GSH) that combated oxidative injury, the increase of

406 glutamate and glutamine might be a consequence of an inhibited GSH synthesis.
407 Depletion of GSH leads to increased level of ROS, causing damage to cellular lipids,
408 proteins, or DNA, producing dysfunction in the body.[26] ROS led to the oxidation of
409 membrane lipid, disrupting both the construction and function of membranes,
410 eventually resulting in the rupture of cell and organelles.[27] The elevated levels of
411 amino acids (leucine, isoleucine and valine) in serum and kidney suggested protein
412 degradation by ROS. Choline and myo-inositol are precursors of all membrane
413 phospholipases,[28] their decrease in kidney of intoxicated rats therefore suggested an
414 accelerated utilization of them for the construction of damaged membranes,
415 representing a self-repair mechanism. Acetyl-glycoproteins (both N-and O-acetyl
416 glycoproteins) are acute phase proteins, acting as inflammatory mediators and could
417 be a response to tissue damage,[29] and thus, the increased concentrations of serum
418 N-acetyl-glycoproteins and O-acetyl-glycoproteins were likely to reflect an
419 inflammatory response.[30] Taurine is one of the most abundant free amino acids present
420 in mammalian tissues. It is reported that taurine treatment could decrease oxidative
421 stress and hepatic prooxidant status; taurine supplementation may cause enhancement
422 in GSH levels by directing cysteine into the GSH synthesis pathway.[31] Trigonelline
423 (TRG) is an alkaloid containing a pyridine ring, showing activities such as
424 anticancer,[32] and improving cognitive function[33] and auditory neuropathy.[34] It has been
425 reported that feeding of TRG may suppress oxidative stress by inhibiting the
426 formation of tumor necrosis factor alpha (TNF-α) and the end-products of advanced
427 glycation, which are known to accelerate the production of ROS via NADPH oxidase;

could slow fat accumulation, resulting in the suppression of ROS formation; may downregulate the gene expressions involved with NADPH oxidase and electron transport chain, indicating that TRG may suppress the formation of ROS.[35] The decreased levels of taurine in urine, serum and kidney and TRG in urine might be a consequence of their over consumption to counteract ROS generated during intoxication. The decreases of renal uridine and adenosine in rats treated with ricinine could be ascribed to the promoted purine and pyrimidine catabolism in kidney by ROS, similar to the CCl_4-induced elevations of purine catabolic product (uric acid) in rat serum,[36, 37] and pyrimidine catabolic product (β-alanine) in rat urine.[38]

Pyruvate is an important intermediate product of glycolysis, the first step in glucose metabolism where pyruvate was generated by the decomposition of glucose, generating a small amount of ATP. Pyruvate can be used to produce acetyl-CoA by pyruvate dehydrogenase complex. Acetyl-CoA enters into TCA cycle, playing a key role in glucose aerobic oxidation and energy production. As important intermediates of TCA cycle, the decreased levels of 2-oxoglutarate (2-OG), succinate and citrate might suggest an inhibition of TCA cycle,[39] the most efficient energy supply pattern. To replenish insufficient energy supply, other means came to the rescue, such as fatty acid β-oxidation. Ketone bodies, comprising acetoacetate, acetone and β-Hydroxybutyrate (3-HB), are well known metabolites of fatty acids in liver mitochondria. Decreased level of serum lipids (LDL/VLDL) and increased level of serum ketone bodies indicated an enhanced lipid oxidation. The increased pyruvate and decreased glucose levels in serum might indicate an enhanced glycolysis to

produce energy.

Phenylalanine (PHE) is an essential amino acid and the precursor of tyrosine. Tyrosine is referred to as a semi-essential or conditionally indispensable amino acid because it can only be synthesized by the hydroxylation of PHE catalyzed by phenylalanine hydroxylase (PAH). The increase of PHE and decrease of tyrosine suggested an inhibition of PAH, which was observed in a previous study on chronic kidney failure.[40] 4-hydroxyphenyllactate (4-HPLA) is a tyrosine metabolite and can be converted into tyrosine. The increased level of 4-HPLA in HD rats might be a result of tyrosine synthesis inhibition, which also suggested nephrotoxicity produced by crude ricinine, since tyrosine has been reported to be reduced substantially in chronic renal impairment.[40, 41]

Alterations in urinary levels of metabolites had at least two reasons, renal and extrarenal perturbations. For example, the increase of urinary lactate and alanine could be ascribed to toxicological impairment of mitochondria in the liver or due to renal tubular injury, affecting renal reabsorption.[42] Elevated urinary lactate and alanine, and decreased serum lactate and alanine confirmed the renal reabsorption impairment. Decreased levels of TCA cycle intermediates in the urine have been observed in a series of studies on $HgCl_2$-induced nephrotoxicity, due to toxin-induced effects on the key enzymes in TCA cycle.[43, 44] The lesion of kidney is also indicated by the remarkable increase of urinary acetate.[45] Thus, the decreased urinary levels of TCA cycle intermediates and serum lactate and alanine, and increased urinary lactate, alanine and acetate might demonstrate the nephrotoxicity induced by crude ricinine.

Urea is the principal end product of protein catabolism in urea cycle, where L-aspartate and amino groups donated by ammonia are converted to urea. Nitrogenous waste is produced mainly by protein catabolism and is removed in the form of urea from the body. Due to special anatomic-functional adaptations of kidney, rodents normally have high urinary urea concentration by an efficient urea concentration mechanism, which keeps the blood urea concentration low. Decreased levels of urinary urea and UUN and increased level of BUN on week 8 in HD rats indicated a dysfunction of nitrogenous waste excretion, thus demonstrating a renal damage induced by crude ricinine. Creatinine is a waste product formed by slow spontaneous degradation of creatine-phosphate.[46] Decrease of urinary excretion of creatinine accompanied with increase of creatinine in serum has also been observed in chronic renal failure, leading to filtration rate falls.[47] This renal failure also happened in crude ricinine intoxicated rats since that decreased creatinine in urine, increased creatinine in both serum and kidney, increased SCR and decreased UCR in biochemistry were also observed in this study. Myo-inositol, one of organic osmolytes, has been reported to be a renal marker of diabetic nephropathy, and to be one of renal markers for detection of renal tubular dysfunction induced by cadmium.[48] Myo-inositol could be a sensitive indicator of impaired renal osmolyte activity caused by melamine and cyanuric acid and ochratoxin A induced toxicity.[49, 50] Notably, ricinine might inhibit two enzymes in the inositol pathway, namely, inositol poly-phosphate 1-phosphatase and inositol monophosphatase, leading to the depletion of inositol levels in tissue,[51] well matched with our results.

Decreased hippurate and increased TMA in urine and decreased TMAO in both urine and serum were observed in HD rats. Decrease of hippurate has multifaceted reasons. Hippurate could be synthesized from benzoic acid in kidney or liver. Its significant decrease in this study thus may be indicative of a metabolic alteration and, even more importantly, of an impairment in its secretion at the level of the proximal tubule.[52] However, the level of hippurate has also been related with the microbial activity and micro floral composition of the colon.[53, 54] It could be produced from the degradation of shikimic acid (quinic acid) by intestinal microorganisms, and could also be synthesized from benzoic acid and phenyl acetic acid, two metabolites produced by bacterial metabolism.[55, 56] Urinary level of hippurate altered in animals exposed to drugs or foods with antimicrobial activity.[57-59] Therefore, the decreased urinary level of hippurate in crude ricinine treated rats may also mirrored a disturbance of the gut microbiota, which was also supported by the significant decrease of TMAO and increase of TMA in HD rats. TMAO is an aliphatic amine and the oxidation product of TMA through the action of gut microbes. It has been reported that the concentration of urinary TMAO gradually increased over the time when germ-free rats were introduced into a normal environment, establishing a stable gut microbiotia gradually.[60]

Conclusion

A ^{1}H NMR based metabolomics approach complemented with histopathological inspection and biochemical assay has been developed to study the chronic toxic effects of crude ricinine in rats. Crude ricinine exhibited obvious nephrotoxicity and produced

severe metabolic alterations which were related with oxidative stress, energy metabolism, amino acid metabolism, renal function and gut bacteria system. This work provided a molecular basis for the chronic toxicity of crude ricinine and showed the power of ^{1}H NMR-based metabolomic approach to study toxicity of drugs dynamically and systematically.

Acknowledgments

This research work was financially supported by the Key Project of National Natural Science Foundation of China (81430092), NSFC grant 81173526, the Priority Academic Program Development of Jiangsu Higher Education Institutions (PAPD), and the Program for Changjiang Scholars and Innovative Research Team in University (PCSIRT-IRT1193).

References

1. X. K. Xie, J. Kirby and J. D. Keasling, *Phytochemistry*, 2012, **78**, 20-28.
2. G. R. Waller, E. K. Nowacki and K. Edmund, *Alkaloid biology and metabolism in plants*, Springer, 1978.
3. V. Bullangpoti, N. Khumrungsee, W. Pluempanupat, Y. Kainoh and U. Saguanpong, *J. Pestic. Sci.*, 2011, **36,** 260-263.
4. M. F. Bigi, V. L. Torkomian, S. T. De Groote, M. J. A. Hebling, O. C. Bueno, F. C. Pagnocca, J. B. Fernandes, P. C. Vieira and M. F. G. Da Silva, *Pest Manag. Sci.*, 2004, **60**, 933-938.
5. M. A. Ramos-López, S. Pérez, G. C. Rodríguez-Hernández, P. Guevara-Fefer and M. A. Zavala-Sánchez, *Afr. J. Biotechnol.*, 2010, **9**.
6. J. Peng, S. Cai, L. Wang, N. Zhao, T. J. Zhang, Z. X. Chen and F. H. Meng, *PloS one*, 2014, **9**, e90416.
7. A. W. Nicholls, E. Holmes, J. C. Lindon, J. P. Shockcor, R. D. Farrant, J. N. Haselden, S. J. Damment, C. J. Waterfield and J. K. Nicholson, *Chem. Res. Toxicol.*, 2001, **14**, 975-987.
8. D. D. Wei, J. S. Wang, P. R. Wang, M. H. Li, M. H. Yang and L. Y. Kong, *J. Pharmaceut. Biomed.*, 2014, **98**, 334-338.
9. D. D. Wei, G. Dong, P. P. Guo, J. S. Wang, M. H. Li, M. H. Yang and L. Y. Kong, *Mol. BioSyst.*, 2014, **10**, 2923-2934.
10. J. K. Nicholson and I. D. Wilson, *Nat. Rev. Drug Discov.*, 2003, **2**, 668-676.

11. J. R. Sheedy, *Metabolomics Tools for Natural Product Discovery*, Springer, 2013, pp. 81-97.
12. A. Craig, J. Sidaway, E. Holmes, T. Orton, D. Jackson, R. Rowlinson, J. Nickson, R. Tonge, I. Wilson and J. Nicholson, *J. Proteome Res.*, 2006, **5**, 1586-1601.
13. P. Li, L. P. Yang and Y. W. Gong, *J. Tradit. Chin. Med.*, 2009, **29**, 153-157.
14. J. K. Nicholson, *Mol. Syst. Biol.*, 2006, **2**.
15. B. W. Tang, J. J. Ding, F. H. Wu, L. Chen, Y. X. Yang and F. Y. Song, *J. Ethnopharmacol.*, 2012, **141**, 134-142.
16. P. P. Guo, J. S. Wang, G. Dong, D. D Wei, M. H. Li, M. H. Yang and L. Y. Kong, *Mol. BioSys.*, 2014, **10**, 2426-2440.
17. G. D. Amico and C. Bazzi, *Curr. Opin. Nephrol. Hy.*, 2003, **12**, 639-643.
18. M. A. Salem, S. A. El‐Habashy, O. M. Saeid, M. M. El‐Tawil and P. H. Tawfik, Pediatric diabetes, 2002, **3**, 37-41.
19. D. Finco and J. Duncan, *J. Am. Vet. Med. Assoc.*, 1976, **168**, 593-601.
20. S. Cuzzocrea, D. P. Riley, A. P. Caputi and D. Salvemini, *Pharmacol. Rev.*, 2001, **53**, 135-159.
21. S. J. Stohs and D. Bagchi, *Free Radical Bio. Med.*, 1995, **18**, 321-336.
22. O. Kumar, K. Sugendran and R. Vijayaraghavan, *Toxicon*, 2003, **41**, 333-338.
23. C. Behl, J. B. Davis, R. Lesley and D. Schubert, *Cell*, 1994, **77**, 817-827.
24. M. Valko, H. Morris and M. T. D. Cronin, *Curr. Med. Chem.*, 2005, **12**, 1161-1208.
25. S. M. Hussain, K. L. Hess, J. M. Gearhart, K. T. Geiss and J. J. Schlager, *Toxicol In Vitro*, 2005, **19**, 975-983.
26. M. Valko, D. Leibfritz, J. Moncol, M. T. D. Cronin, M. Mazur and J. Telser, *Int. J. Biochem. Cell B.*, 2007, **39**, 44-84.
27. P.-R. Wang, J.-S. Wang, M.-H. Yang and L.-Y. Kong, *J. Pharmaceut. Biomed.*, 2014, **88**, 106-116.
28. M. Yang, S. Wang, F. Hao, Y. Li, H. Tang and X. Shi, *Talanta*, 2012, **88**, 136-144.
29. J. Saric, J. V. Li, J. R. Swann, J. Utzinger, G. Calvert, J. K. Nicholson, S. Dirnhofer, M. J. Dallman, M. Bictash and E. Holmes, *J. Proteome Res.*, 2010, **9**, 2255-2264.
30. M. Bhatia and S. Moochhala, *J. Pathol.*, 2004, **202**, 145-156.
31. E. B. Kalaz, J. Çoban, A. F. Aydın, I. Doğan-Ekici, S. Doğru-Abbasoğlu, S. Öztezcan and M. Uysal, *J. Physiol. Biochem.*, 2013, 1-11.
32. N. Hirakawa, R. Okauchi, Y. Miura and K. Yagasaki, *Biosci. Biotechnol. Biochem.*, 2005, **69**, 653-658.
33. C. Tohda, T. Kuboyama and K. Komatsu, *Neurosignals*, 2005, **14**, 34-45.
34. B. N. Hong, T. H. Yi, S. Y. Kim and T. H. Kang, *Biol. Pharm. Bull.*, 2009, **32**, 597-603.
35. O. Yoshinari, A. Takenake and K. Igarashi, *J. Med. food*, 2013, **16**, 34-41.
36. B. Soni, N. P. Visavadiya and D. Madamwar, *Toxicology*, 2008, **248**, 59-65.
37. Y. Ohta, M. Kongo-Nishimura, Y. Imai and T. Kishikawa, *J. Clin. Biochem. Nutr.*, 2003, **33**, 83-93.
38. Y. P. Lin, D. Y. Si, Z. P. Zhang and C. X. Liu, *Toxicology*, 2009, **256**, 191-200.
39. M. I. Shariff, A. I. Gomaa, I. J. Cox, M. Patel, H. R. Williams, M. M. Crossey, A. V. Thillainayagam, H. C. Thomas, I. Waked, S. A. Khan and S. D. Taylor-Robinson, *J. Proteome Res.*, 2011, **10**, 1828-1836.
40. J. D. Kopple, *J. Nutr.*, 2007, **137**, 1586S-1590S.
41. R. E. Williams and E. A. Lock, *Toxicology*, 2004, **201**, 231-238.
42. C. F. Lu, Y. W. Wang, Z. G. Sheng, G. Liu, Z. Fu, J. Zhao, J. Zhao, X. Z. Yan, B. Z. Zhu and S. Q. Peng, *Toxicol. Appl. Pharm.*, 2010, **248**, 178-184.
43. J. K. Nicholson, J. A. Timbrell and P. J. Sadler, *Mol. Pharmacol.*, 1985, **27**, 644-651.
44. E. Holmes, F. W. Bonner, K. P. R. Gartland and J. K. Nicholson, *J. Pharmaceut. Biomed.*, 1990, **8**, 959-962.
45. K. P. Gartland, F. W. Bonner, J. A. Timbrell and J. K. Nicholson, *Arch. Toxicol.*, 1989, **63**, 97-106.
46. M. Wyss and R. Kaddurah-Daouk, *Physiol. Rev.*, 2000, **80**, 1107-1213.

47. R. Goldman, *Exp. Biol. Med.*, 1954, **85**, 446-448.
48. D. Suvagandha, M. Nishijo, W. Swaddiwudhipong, R. Honda, M. Ohse, T. Kuhara, H. Nakagawa and W. Ruangyuttikarn, *Inter. J. Env. Res. Pub. Heal.*, 2014, **11**, 3661-3677.
49. T. H. Kim, M. Y. Ahn, H. J. Lim, Y. J. Lee, Y. J. Shin, U. De, J. Lee, B. M. Lee, S. Kim and H. S. Kim, *Arch. Toxicol.*, 2012, **86**, 1885-1897.
50. M. Sieber, S. Wagner, E. Rached, A. Amberg, A. Mally and W. Dekant, *Chem. Res. Toxicol.*, 2009, **22**, 1221-1231.
51. P. E. Brandish, M. Su, D. J. Holder, P. Hodor, J. Szumiloski, R. R. Kleinhanz, J. E. Forbes, M. E. McWhorter, S. J. Duenwald and M. L. Parrish, *Neuron.*, 2005, **45**, 861-872.
52. C. Zuppi, I. Messana, F. Forni, C. Rossi, L. Pennacchietti, F. Ferrari and B. Giardina, *Clin. Chim. Acta*, 1997, **265**, 85-97.
53. A. W. Nicholls, R. J. Mortishire-Smith and J. K. Nicholson, *Chem. Res. Toxicol.*, 2003, **16**, 1395-1404.
54. R. E. Williams, H. W. Eyton-Jones, M. J. Farnworth, R. Gallagher and W. M. Provan, *Xenobiotica*, 2002, **32**, 783-794.
55. A. N. Phipps, J. Stewart, B. Wright and I. D. Wilson, *Xenobiotica*, 1998, **28**, 527-537.
56. J. Delaney, W. A. Neville, A. Swain, A. Miles, M. S. Leonard and C. J. Waterfield, *Biomarkers*, 2004, **9**, 271-290.
57. Y. L. Wang, H. R. Tang, J. K. Nicholson, P. J. Hylands, J. Sampson and E. Holmes, *J. Agr. Food Chem.*, 2005, **53**, 191-196.
58. C. A. Daykin, J. P. M. Van Duynhoven, A. Groenewegen, M. Dachtler, J. M. M. Van Amelsvoort and T. P. J. Mulder, *J. Agr. Food Chem.*, 2005, **53**, 1428-1434.
59. N. J. Waters, C. J. Waterfield, R. D. Farrant, E. Holmes and J. K. Nicholson, *J. Proteome Res.*, 2006, **5**, 1448-1459.
60. J. K. Nicholson and I. D. Wilson, *Nat. Rev. Drug Discov.*, 2003, **2**, 668-676.